

Spectroscopic and Structural Properties of Valine Gramicidin A in Monolayers at the Air-Water Interface

Hugo Lavoie,* Daniel Blaudez,[†] David Vaknin,[‡] Bernard Desbat,[§] Benjamin M. Ocko,[¶] and Christian Salesses*

*Département de Chimie-Biologie, Université du Québec à Trois-Rivières, Trois-Rivières, Québec G9A 5H7, Canada; [†]Centre de Physique Moléculaire Optique et Hertzienne and [§]Laboratoire de Physico-Chimie Moléculaire, Université Bordeaux I, 33405 Talence, France;

[‡]Ames Laboratory and Department of Physics, Iowa State University, Ames, Iowa 50011 USA; and [¶]Brookhaven National Laboratory, Department of Physics, Upton, New York 11973 USA

ABSTRACT Monomolecular films of valine gramicidin A (VGA) were investigated in situ at the air-water interface by x-ray reflectivity and x-ray grazing incidence diffraction as well as polarization modulation infrared reflection absorption spectroscopy (PM-IRRAS). These techniques were combined to obtain information on the secondary structure and the orientation of VGA and to characterize the shoulder observed in its π -A isotherm. The thickness of the film was obtained by x-ray reflectivity, and the secondary structure of VGA was monitored using the frequency position of the amide I band. The PM-IRRAS spectra were compared with the simulated ones to identify the conformation adopted by VGA in monolayer. At large molecular area, VGA shows a disordered secondary structure, whereas at smaller molecular areas, VGA adopts an anti-parallel double-strand intertwined $\beta^{5,6}$ helical conformation with 30° orientation with respect to the normal with a thickness of 25 Å. The interface between bulk water and the VGA monolayer was investigated by x-ray reflectivity as well as by comparing the experimental and the simulated PM-IRRAS spectra on D₂O and H₂O, which suggested the presence of oriented water molecules between the bulk and the monolayer.

INTRODUCTION

It has long been suggested that proteins can denature upon spreading at the air-water interface (for a review, see MacRitchie 1978, 1986). Gidalevitz et al. (1999) have shown by x-ray reflectivity that this indeed is the case for glucose oxidase, urease, and alcohol dehydrogenase. Wu et al. (1999) have also shown that annexin V experiences a marked alteration of its secondary structure in the absence of lipid. Although denaturation usually occurs upon spreading the protein film, it has been shown recently that by manipulating external factors such as surface pressure, subphase conditions (ion concentration and pH), and spreading procedures that the native structure of proteins can be maintained at the air-water interface. This in fact was demonstrated by Gallant et al. (1998), Blaudez et al. (1999), and Lavoie et al. (1999) who have shown by in situ infrared spectroscopy that the native secondary structure of the membrane proteins photosystem II core complex, bacteriorhodopsin and rhodopsin, respectively, can be retained in monolayers at the air-water interface. However, all of those proteins contain extensive secondary structures, which complicate the understanding of the mechanism taking place during spreading and compression of polypeptides. In this paper, we have made use of the simple aliphatic peptide gramicidin to facilitate the analysis of this process and to improve our understanding of its behavior upon compression.

Linear gramicidin is a hydrophobic antibiotic polypeptide composed of 15 hydrophobic amino acids in D- and L-alternate conformers with the following sequence: formyl-L-X-gly-L-ala-D-leu-L-ala-D-val-L-val-D-val-L-trp-D-leu-L-trp-D-leu-L-trp-D-leu-L-trp-ethanolamine where X represents either valine or isoleucine. Whether amino acid 11 is tryptophan, phenylalanine, or tyrosine, gramicidins are called A, B, or C, respectively (Sarges and Witkop, 1965). In bilayers, it is well known that valine gramicidin A (VGA) forms ion channels that allow conduction of monovalent cations through lipid membranes (Hladky and Haydon, 1972; Urban et al., 1978, 1980). Several structural arrangements of the polypeptide that show the formation of these channels have been proposed (Langs, 1988; Salemme, 1988; Wallace, 1998). Channel formation has been explained in terms of two helical monomers placed end to end or in terms of parallel or antiparallel intertwined double helices (Wallace, 1986, 1998; Quist, 1998). The conformation of VGA depends on the type of solvent used and the monovalent ions present in the solution (Wallace, 1986; LoGrasso et al., 1988; Killian, 1992). However, in monolayers, divergent results have been reported on the conformation and orientation of VGA at the air-water interface (Dhathathreyan et al., 1988; Ulrich and Vogel, 1999). The shoulder region ($\pi = 15\text{--}17 \text{ mN m}^{-1}$) in the surface pressure isotherm of VGA has been attributed to different phenomena such as structural phase transition, cluster formation, reorientation of the molecules, reorganization of the film or the molecules, molecular structure change, or transition from monomer to dimer (Kemp and Wenner, 1976; Tournois et al., 1989).

In situ techniques to probe the monomolecular layers at the air-water interface are now well established. For in-

Submitted December 3, 2001 and accepted for publication August 13, 2002.

Address reprint requests to Dr. Christian Salesses, Département de Chimie-Biologie, Université du Québec à Trois-Rivières, Trois-Rivières, Québec Canada, G9A 5H7. Tel.: 819-376-5011; Fax: 819-376-5057; E-mail: christian_salesse@uqtr.ca.

© 2002 by the Biophysical Society

0006-3495/02/12/01/00 \$2.00

stance, x-ray and neutron reflectivity, and x-ray grazing incidence diffraction (XGID) of free liquid surfaces allow determination of the electron density across the interface and two-dimensional arrangements in the film on a molecular length scale (Als-Nielsen and Kjaer, 1989). Infrared reflection absorption spectroscopy (IRRAS) (Dluhy and Mendelsohn, 1988) and polarization modulation (PM)-IRRAS (Blaudez et al., 1993) are additional powerful tools that were recently used to extract information on the secondary structure and orientation of peptide and protein monolayers at the air-water interface (Dluhy et al., 1989; Flach et al., 1994, 1996; Cornut et al., 1996; Gallant et al., 1998; Castano et al., 1999, 2000; Lavoie et al., 1999; Ulrich and Vogel, 1999; Wu et al., 1999; Dieudonne et al., 2001). In the present study, we combined the use of x-ray scattering techniques (x-ray reflectivity and XGID) and PM-IRRAS to shed light on the structure and organization of VGA in monolayer at various points along its π -A isotherm. The effect of the VGA film on the organization of interfacial water is also discussed.

MATERIALS AND METHODS

Surface pressure isotherms

High-purity valine gramicidin A was generously provided by Dr. J. Morell (National Institutes of Health, Bethesda, MD). VGA was dissolved in Megasolv HPLC-grade chloroform (Omega, Lévis, Canada), and aliquots of this solution were spread onto Millipore water (18.2 M Ω cm). Surface pressure was measured with a Wilhelmy-type balance (M-balance, R&K, Mainz, Germany). The film was compressed either continuously or stepwise at a rate of 0.05 nm² per monomer per minute with no marked difference between the resulting isotherms.

X-ray reflectivity and XGID measurements

X-ray reflectivity and XGID measurements were performed in situ at the air-water interface on the X22B liquid surface diffractometer at the National Synchrotron Light Source, Brookhaven National Laboratory, which has been described in detail elsewhere (Als-Nielsen and Pershan, 1983). An x-ray wavelength $\lambda = 1.527 \pm 0.006$ Å was selected by Bragg reflection from the (111) plane of a germanium crystal. The intensity of the incident beam, before reaching the sample, was continuously monitored to account for all kinds of primary beam fluctuations. To reduce liquid-surface waves during measurements, a glass plate was positioned in the trough under the x-ray beam footprint. The subphase depth above the glass plate was kept at ~ 0.3 mm thick. A dynamic vibration isolation system (JRS MOD-2 Affoltern, Switzerland) was used to eliminate mechanical vibrations. The Langmuir trough was contained in an airtight aluminum enclosure with Kapton windows, and its temperature was constantly maintained at 20°C. After spreading the monolayer, the sealed container was flushed with helium for ~ 1 h before x-ray measurements to reduce background caused by air scattering. For diffraction measurements, Soller slits with the leaves oriented vertically were placed just before the detector, yielding in-plane resolution function with a full width of ~ 0.01 Å⁻¹.

PM-IRRAS measurements

PM-IRRAS spectra were recorded at the air-water interface by co-addition of 800 scans at a resolution of 8 cm⁻¹ using a Nicolet 740 spectrometer

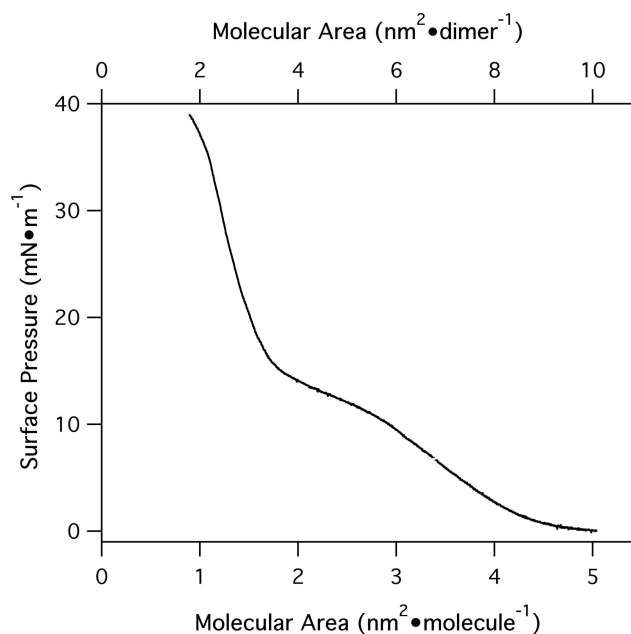


FIGURE 1 Surface pressure isotherm of VGA at 20°C on pure water.

following the experimental procedure previously described (Blaudez et al., 1993). The PM-IRRAS spectra of covered surface, S_{film} , as well as that of the bare water (H_2O or D_2O), S_{w} , were measured, and the normalized difference $\Delta S = [S_{\text{film}} - S_{\text{w}}]/S_{\text{w}}$ is presented. On dielectric substrates, PM-IRRAS presents a specific surface selection rule, such that a transition dipole moment lying in the plane or perpendicular to the surface yields a positive or a negative absorption band signal, respectively, with respect to the baseline (Blaudez et al., 1996). For an intermediate orientation of the transition dipole moment, the two contributions are competing and the absorption band vanishes when the transition dipole moment is tilted at $\sim 39^\circ$ from the surface normal of the water subphase (Blaudez et al., 1996).

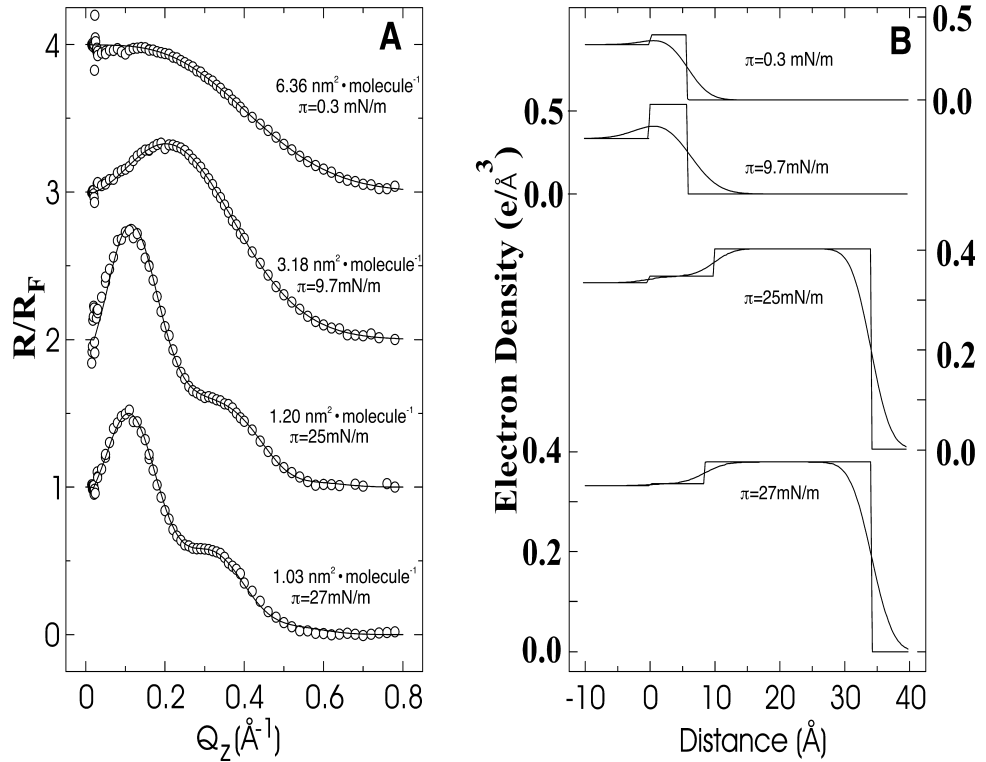
RESULTS

Surface pressure, x-ray reflectivity, and thickness measurements

The surface pressure (π -A) isotherm of pure VGA at the air-water interface presented in Fig. 1 is in agreement with previously published data (Kemp and Wenner, 1976; Mau et al., 1987; Tournois et al., 1989; Ducharme et al., 1996). A liquid-like phase extends from the onset of the surface pressure (~ 4.75 nm² per molecule) to the characteristic shoulder, which occurs between ~ 12.5 and 15 mN m⁻¹ (between 2.5 and 1.8 nm² per molecule). An inflection is then observed at the end of the shoulder, and the film becomes highly incompressible and rigid.

Fig. 2 A shows typical normalized x-ray reflectivity curves of VGA at different surface pressures as a function of the momentum transfer Q_z . The measured reflectivity curves $R(Q_z)$ were normalized to the Fresnel reflectivity $R_{\text{F}}(Q_z)$ calculated for an ideally flat water surface with an electron density, $\rho_{\text{w}} = 0.334$ e/Å³. The solid lines are the best-fit calculated reflectivities using the scattering length

FIGURE 2 (A) X-ray reflectivity of VGA at 20°C normalized to the reflectivity of pure water subphase. The solid line is calculated from an electron density profile shown in B. The step-like line illustrates the ideally sharp interfaces that are Gaussian-smearred because of surface roughness to yield the smooth line. (B) A depiction showing the correspondence between the electron density and the molecular arrangement.



density profiles $\rho(z)$ shown in Fig. 2 B. These profiles consist of step functions (box model) that are convoluted with a Gaussian of width σ (surface roughness) to yield smooth error functions (Als-Nielsen and Kjaer, 1989). In refining the model, it is initially assumed that the film consists of a single homogeneous slab, and a second slab is added only if it improves the quality of the fit. The thickness of the box, the electron density, and the surface roughness are the free variables in the refinement (Als-Nielsen and Kjaer, 1989). Fig. 2 B shows that the best fit is obtained with the one-slab model at low surface pressures (below $\sim 10 \text{ mN m}^{-1}$), whereas at high surface pressures a second slab between the monolayer and the substrate has to be included. The structural parameters of the two-box model for VGA on water as determined from x-ray reflectivity measurements is presented in Table 1.

The monolayer thickness obtained from the x-ray reflectivity measurements at different surface pressures is shown in Fig. 3. This figure shows that the film thickness remains almost unchanged at low surface pressure (from 0 to 10 mN m^{-1} or 5 to 3 nm^2 per molecule). This behavior is completely different from that of amphiphilic molecules, which straighten up regularly upon compression. It can be interpreted in terms of a reorganization of the secondary structure of VGA as suggested by the PM-IRRAS data (see below). The thickness of the film at low surface pressures ($d \approx 6\text{--}9 \text{ \AA}$) is significantly smaller than the minimal dimension of VGA in the β -helical conformation as determined by its crystal structure (the smaller axis of VGA is $14\text{--}16 \text{ \AA}$, whereas the larger one is $26\text{--}30 \text{ \AA}$ (see inset of Fig. 3) (Langs, 1988; Wallace and Ravikumar, 1988). As the monolayer is compressed to high surface pressures, Fig.

F3

T1

TABLE 1 Structural parameters of the two-box model for VGA on water as determined from x-ray reflectivity measurements

π (mN m^{-1})	A (nm^2 per molecule)	d_{water} (\AA)	ρ_{water} ($e/\text{\AA}^3$)	d_{VGA} (\AA)	ρ_{VGA} ($e/\text{\AA}^3$)	N_{water}
0.3	6.36			$5.7^{+2.8}_{-2.0}$	$0.393^{-0.035}_{+0.08}$	41^{+52}_{-30}
1.8	5.15			$8.1^{+2.9}_{-4.1}$	$0.383^{+0.020}_{+0.148}$	58^{+46}_{-50}
9.7	3.18			$9.0^{+1.0}_{-1.0}$	$0.416^{-0.015}_{+0.021}$	18^{+8}_{-8}
13.8	2.20			$10.0^{+1.0}_{-1.0}$	$0.416^{-0.013}_{+0.023}$	-6^{+6}_{-6}
15.0	2.10			$11.5^{+1.0}_{-1.0}$	$0.406^{+0.02}_{-0.015}$	
25.0	1.20	10.1 ± 5	0.347 ± 0.005	$24.2^{+1.0}_{-1.0}$	$0.402^{-0.015}_{+0.02}$	
27.0	1.03	8.5 ± 5	0.344 ± 0.005	$25.1^{+1.0}_{-1.0}$	$0.389^{-0.01}_{+0.01}$	

One box model is sufficient for the description of VGA, whereas at high surface pressures an additional layer is required to get the best fit to the data. N_{water} corresponds to the number of water molecules that are integrated in the VGA box. π , surface pressure; A , area per molecule; ρ , electronic density; N_{water} , number of water molecules.

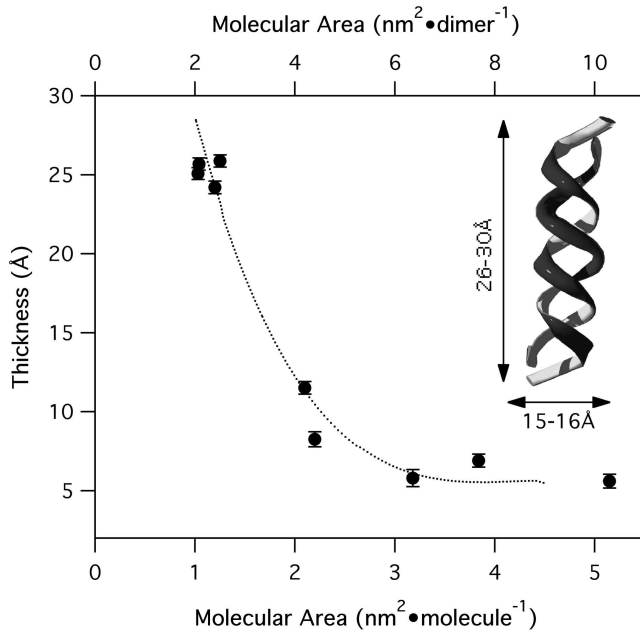


FIGURE 3 Thickness of VGA on pure water versus the molecular area as determined by x-ray reflectivity. The inset shows a sketch of the structure of VGA with the dimension of its small and large axis from its crystal structure (Langs, 1988).

3 shows an abrupt change in film thickness from $d \approx 6 - 9 \text{ \AA}$ to $d \approx 25 \text{ \AA}$. This latter thickness value is slightly smaller than the one of $26-30 \text{ \AA}$ found for the larger axis of VGA in the β -helical conformation determined from the three-dimensional crystal structure (see inset of Fig. 3) (Langs, 1988; Wallace and Ravikumar, 1988) and suggests

that VGA is not oriented parallel to the normal of the monolayer, which is consistent with the PM-IRRAS data.

To correlate the electron density (Fig. 2 B) with the molecular density at the interface, we proceeded by calculating the number of electrons per molecule assuming an average molecular area A , as follows:

$$N_{\text{ref}} = A \int \rho(z) dz \quad (1)$$

The empirical formula for VGA yields a total number of electrons per monomer, $N_{\text{total}} = 1010$. For comparison, at high surface pressures $\pi \geq 20 \text{ mN m}^{-1}$, Eq. 1 yields $N_{\text{ref}} = 1009 \pm 50$ electrons per monomer, which is in good agreement with N_{total} . However, this result indicates the lack of bound water molecules in any region of VGA. In particular, it suggests that the channel is void of water molecules. By contrast, at very low surface pressures, $N_{\text{ref}} = 1432 \pm 100$ electrons, indicating that the film consists of VGA plus water molecules, which is also consistent with the N-H to N-D exchange measured by PM-IRRAS on D_2O (see below). This result independently supports the view of an unfolded VGA at large molecular areas with a large number of bound water molecules.

XGID measurements

Fig. 4 shows XGID versus in-plane momentum transfer (Q_{xy}) of VGA at 25 mN m^{-1} , with two peaks at $Q_{xy}^1 = 0.459 \text{ \AA}^{-1}$ and $Q_{xy}^2 = 1.159 \text{ \AA}^{-1}$. The scan presented in this figure is obtained after subtracting a similar scan from bare water surface under similar conditions as for the VGA

F4

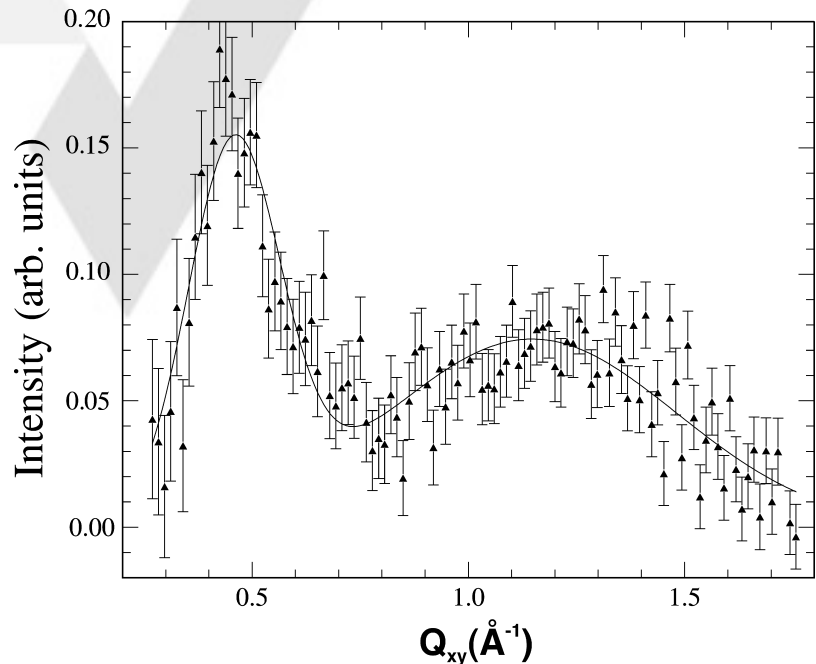
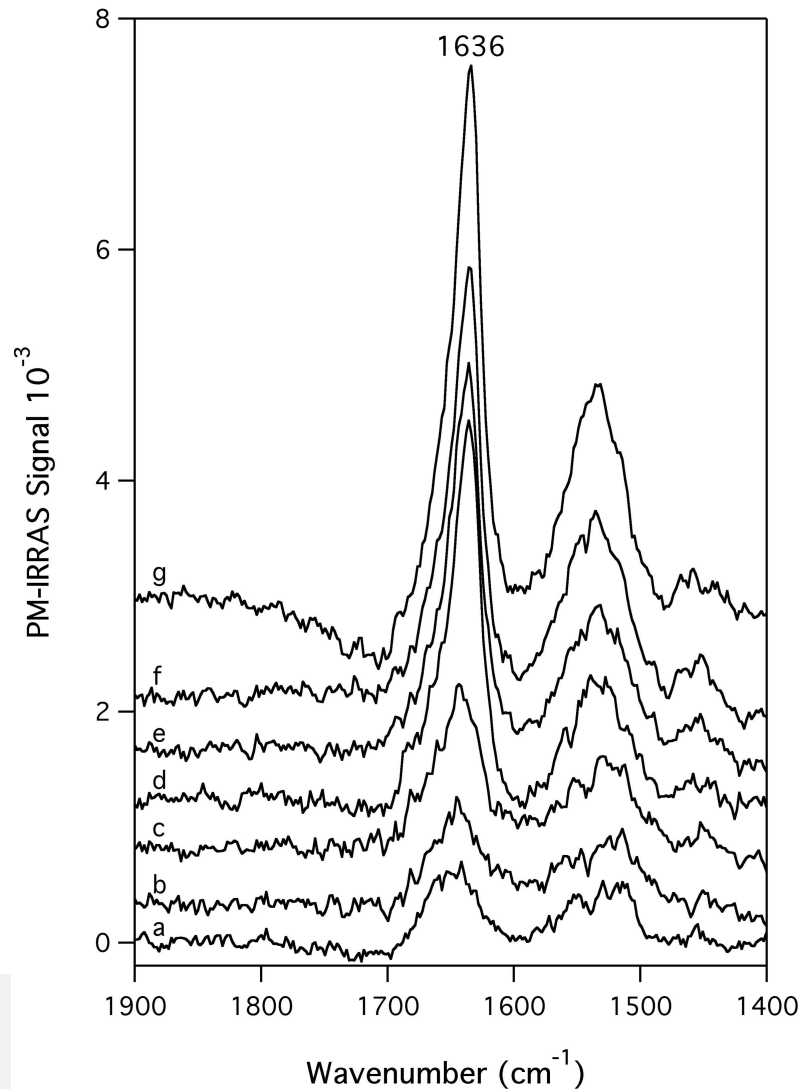


FIGURE 4 XGID of VGA in situ at the air/water interface at a surface pressure of 25 mN m^{-1} ($1.4 \text{ nm}^2/\text{molecule}$). The sharper peak (at $Q_{xy}^1 = 0.459 \text{ \AA}^{-1}$) is because of the short-range in-plane order of the folded protein.

AQ: F

FIGURE 5 PM-IRRAS spectra of VGA in situ at the air/water interface on pure H₂O at different surface pressures: 0 (a), 5 (b), 10 (c), 15 (d), 20 (e), 30 (f), and 40 (g) mN m⁻¹.



monolayer. Similar scans at pressures that are smaller than 20 mN m⁻¹ did not yield any detectable signals. The d -spacing associated with the first peak is $2\pi/Q_{xy}^1 = 13.69$ Å, and the full width at half-maximum $\Delta Q_{xy}^1 = 0.16$ Å⁻¹, indicating short-range correlations in the film. The correlation length extends over two to three molecular lengths, which in general is characteristic of an amorphous solid or a liquid. Assuming that the short-range order is hexagonal in nature, the average molecular area extracted from the diffraction is $A_{x\text{-ray}} = 2.17 \pm 10$ nm² at 25 mN m⁻¹. This molecular area is approximately twice as large as the one obtained from the isotherm at that surface pressure (Fig. 1). It should be noted here that, in general, the molecular area presented in isotherms is calculated per monomer. This leads us to propose that the observed diffraction peak corresponds to the ordering of dimers at the air-water interface. The in-plane d -spacing together with the thickness of the film extracted from the reflectivity both imply that the polypeptide consists of an intertwined dimer that is folded

most likely in a tubular shape, which is consistent with the PM-IRRAS data (see below).

PM-IRRAS measurements on pure H₂O

Fig. 5 shows PM-IRRAS spectra in the 1900–1400-cm⁻¹ spectral range from a VGA monolayer on pure water at different surface pressures. At low surface pressures (below 10 mN m⁻¹), the maximum of the amide I band at 1645 cm⁻¹ indicates a disordered secondary structure, namely, an almost completely unfolded polypeptide (Goormaghtigh et al., 1990), in agreement with the x-ray reflectivity data (see above). However, the orientation of the VGA molecules is probably not entirely isotropic because the ratio of the amide I/amide II intensity bands of 1.045 is much lower than the value of 1.920 obtained in bulk (Dhathathreyan et al., 1988). Considering the surface selection rule of PM-IRRAS at the air-water interface, this ratio of 1.045 indi-

F5

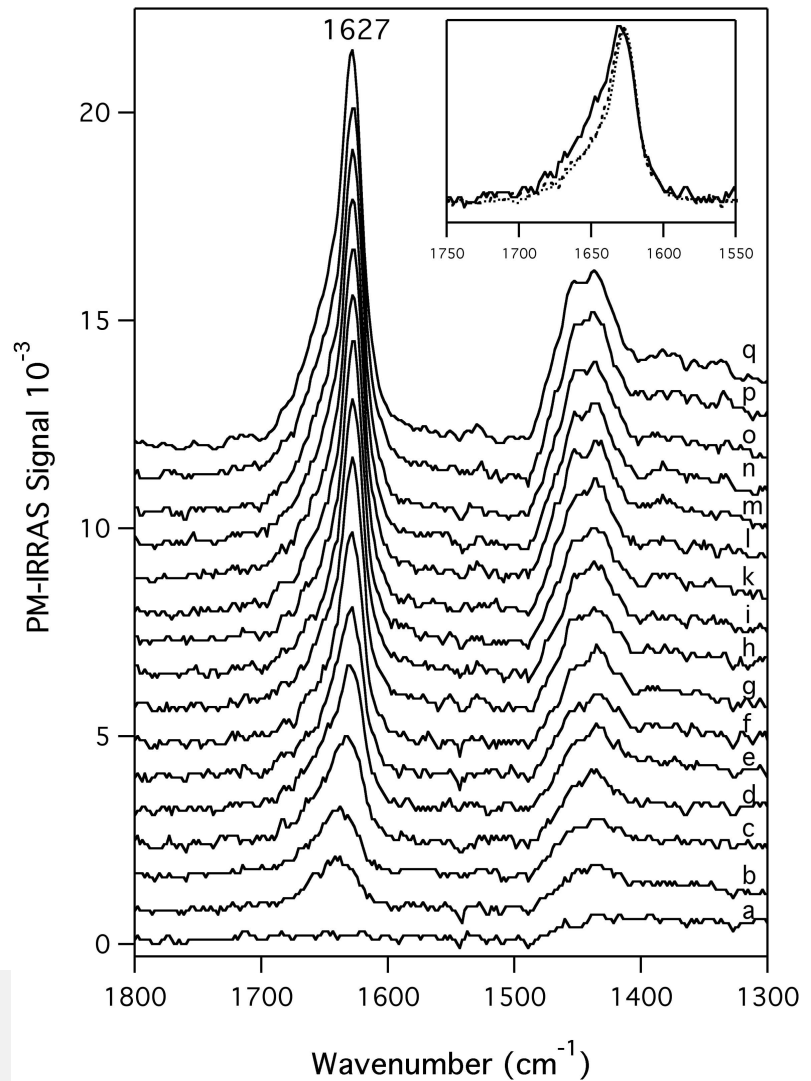


FIGURE 6 PM-IRRAS spectra of VGA in situ at the air/water interface on pure D₂O at different surface pressures: 0.8 (a), 1.6 (b), 5 (c), 9 (d), 12 (e), 13 (f), 15 (g), 16.5 (h), 18.5 (i), 22 (j), 26 (k), 30 (l), 35 (m), 40 (n), 45 (o), 52 (q) mN m⁻¹. The inset shows normalized PM-IRRAS spectra of VGA on pure D₂O at 12 mN m⁻¹ (—), 15 mN m⁻¹ (···), and 40 mN m⁻¹ (— —).

AQ: G

cates that the transition dipole moment of the amide II mode is more preferentially oriented in the interface plane than that of the amide I mode. At 15 mN m⁻¹, above the inflection point at the end of the shoulder in the π -A isotherm, the amide I band becomes sharper and shifts to 1636 cm⁻¹. Such a shift has also been observed by Ulrich and Vogel (1999). This shift of the peak position is indicative of a reorganization of the secondary structure of VGA. The gradual shift of the peak and its narrowing show that the folding process takes place over a wide range of molecular areas. At a surface pressure of 40 mN m⁻¹, a negative component can be observed in the PM-IRRAS spectrum at \sim 1700 cm⁻¹, which is associated with the $\delta(\text{OH}_2)$ deformation mode of the liquid water as observed by Ulrich and Vogel (1999). This component originates from an optical effect (Grandbois et al., 2000) and can also be partly caused by restructured water molecules underneath the monolayer (Blaudez et al., 1996). To eliminate this contribution, which interferes with both the peak posi-

tion and the integrated intensity of the amide I band, PM-IRRAS spectra of VGA in monolayer were also conducted on D₂O subphase. The use of a D₂O subphase is also particularly important for the spectral simulations presented hereafter.

PM-IRRAS measurements on pure D₂O

Fig. 6 shows the PM-IRRAS spectra of a VGA monolayer obtained at different surface pressures on a pure D₂O subphase. The disappearance of the amide II band (combination of $\delta\text{N-H}$ and $\nu\text{C-N}$) and its replacement by the amide II' (pure $\nu\text{C-N}$) located at 1440 cm⁻¹ proves the complete exchange of hydrogen atoms by deuterium atoms during the course of the experiment. Moreover, no extra signal caused by H₂O in exchange with D₂O subphase in the 1500- and 1800-cm⁻¹ range is visible. At low surface pressure ($\pi = 0.8$ mN m⁻¹), the amide II' band is hardly observed,

F6

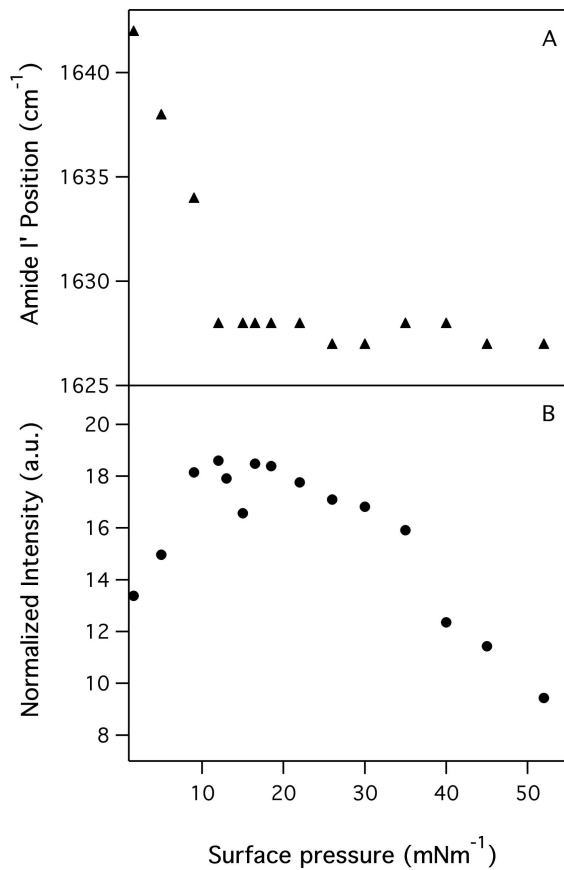


FIGURE 7 (A) Peak position of the amide I' band as a function of the molecular area; (B) Intensity of the amide I' band normalized to the in-plane density as a function of the surface pressure (mN m⁻¹).

whereas the amide I' is not observed at all. The amide I' becomes predominant as π increases, as observed for the monolayer on H₂O. However, we would like to emphasize that, compared with H₂O, the main modification occurring in the spectrum with the use of the D₂O subphase concerns the increase of the amide I intensity by a factor of ~ 2 . We will see that simulations allow us to explain this behavior (see below). The peak position at 1627 cm⁻¹ and the presence of a shoulder near 1660 cm⁻¹ suggest that VGA adopts an antiparallel $\beta^{5,6}$ -helical conformation at high surface pressure, in agreement with results of LB films of VGA on glass plates (Dhathathreyan et al., 1988).

Fig. 7 A shows the amide I' peak position of VGA on D₂O as a function of surface pressure. There are two distinct regions upon compression. The amide I' band frequency shifts gradually from 1642 to 1628 cm⁻¹ with increasing surface pressure from 0 to 13 mN m⁻¹ and then further shifts to reach a stable value of 1627 cm⁻¹ at 15 mN m⁻¹. Ulrich and Vogel (1999) have measured one PM-IRRAS spectrum of VGA at 14 mN m⁻¹ on D₂O. The maximum of their amide I' band is located at 1630 cm⁻¹, in good agreement with our data. The first region between 0 and 15

mN m⁻¹ shows that VGA undergoes a change in secondary structure. This rearrangement takes place all along the compression and ends at a surface pressure of 15 mN m⁻¹, i.e., slightly after the end of the shoulder on the π -A isotherm (Fig. 1). The inset of Fig. 6 shows normalized spectra at 12, 15, and 40 mN m⁻¹. It can be seen that no further shift of the amide I' band is observed from 15 mN m⁻¹. In addition, a component at ~ 1645 cm⁻¹ can be seen in the spectra up to 13 mN m⁻¹, which corresponds to the position of the unfolded peptide. These observations further stress that the change in secondary structure of VGA is terminated at 15 mN m⁻¹. Further compression does not provide any change in the secondary structure of VGA. This demonstrates that the shoulder does not correspond to a phase transition but is essentially caused by VGA secondary structure reorganization.

Fig. 7 B shows the integrated intensity of the amide I' band normalized to the in-plane density, as a function of the surface pressure. The intensity of this band shows a broad maximum in the 10- and 20-mN m⁻¹ range. Considering the amide I' peak position (Fig. 7 A), the three succeeding regimes observed in Fig. 7 B can be interpreted as follows. 1) The first increase between 0 and 10 mN m⁻¹ can be attributed to a reorganization of the secondary structure of VGA with the formation of intertwined β -helix, in good agreement with the shift of the amide I' peak position observed by PM-IRRAS (see Fig. 7 A). 2) The plateau between 10 and 20 mN m⁻¹ in Fig. 7 B shows that only the surface density of VGA changes with compression in this surface pressure range. 3) The decrease after 20 mN m⁻¹ suggests that the intertwined β -helices, which are initially likely flat at the interface, are tilting with the compression of the film.

Simulation of the PM-IRRAS spectra

To determine the secondary structure and the orientation of VGA at high surface pressure, we have carried out simulations of PM-IRRAS spectra using the extensive vibrational calculations of the six known conformations of VGA reported by Naik and Krimm (1986). We have assumed the validity of these calculated values. This remarkable work has provided, for each conformation, the frequency positions of each amide I component and their intensity in the three directions of the molecular reference frame (u , v , and w). We have used these values to build the anisotropic optical constants of each conformation (k_u , k_v , and k_w). As vibrational calculation gives only the integrated intensity of a mode, we have attributed a Lorentzian band shape and a width at half-intensity of 30 cm⁻¹ to each component. The real part of the complex refractive indices (n_u , n_v , and n_w) has been obtained by Kramers-Kronig inversion of the extinction coefficients k_u , k_v , and k_w . Then, these optical constants have been expressed in the monolayer frame (x , y , and z) with the condition for the film to be uniaxial ($n_u =$

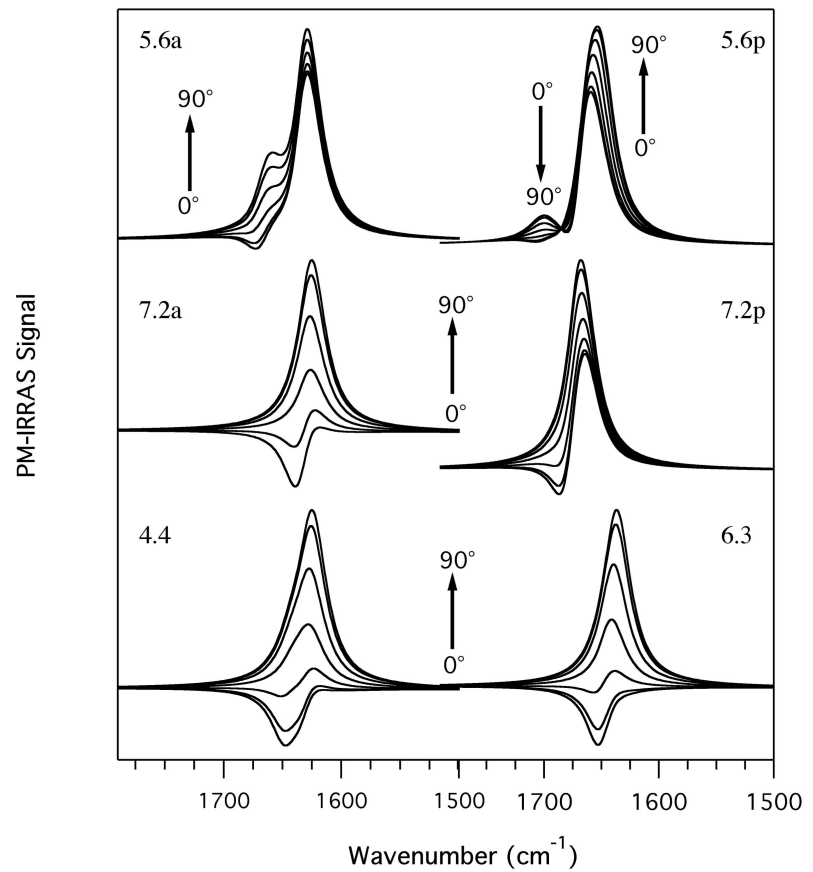


FIGURE 8 PM-IRRAS spectra simulation of six different gramicidin secondary structures. Simulation of each set of conformations is performed at different tilt angles of the transition dipole moment (0° to 90°).

$n_y n_z$ and $k_x = k_y k_z$). A general software previously described (Buffeteau et al., 1999) has been used to obtain the simulated PM-IRRAS spectra.

Fig. 8 shows the simulated spectra of the six known conformations at different tilt angles (from 0° to 90°) with respect to the surface normal in the amide I spectral region. The optical constants have been slightly perturbed to get a simulated spectrum with an intensity as close as possible from the experimental spectrum on D_2O at 40 mN m^{-1} . In all cases, the thickness has been fixed to 25 \AA as determined by x-ray reflectivity and the D_2O optical constants were those given by Bertie et al. (1989). Several conformations can be discarded by comparing the experimental spectrum at 40 mN m^{-1} (Fig. 6) and the simulated spectra shown in Fig. 8. It can first be seen that the band position of several spectra is not consistent with the experimental data. This is the case of the parallel double strand $\beta^{5.6}$ helices (5.6p) and $\beta^{7.2}$ (7.2p) with an amide I' band position of 1659 and 1673 cm^{-1} , respectively. For the remaining conformations, the $\beta^{7.2}$ (7.2a), $\beta^{6.3}$ (6.3), and $\beta^{4.4}$ (4.4) helices can be ruled out because their amide I' band does not show any shoulder, contrary to the experimental spectrum. Finally, the best fit for the main band at 1627 cm^{-1} on the experimental spectrum is obtained with the anti-parallel $\beta^{5.6}$ -helical (5.6a) conformation. In contrast, Ulrich and Vogel (1999) could

not distinguish between the $\beta^{5.6a}$ and $\beta^{6.3}$ conformations mainly because their spectra were noisier than in the present study and they did not have thickness data to implement their simulations. Moreover, the antiparallel $\beta^{5.6}$ conformation is the only structure that presents a dichroic ratio near the unit value for its main vibrational band. The quasi-unit value is a necessary condition to explain the small change observed in the PM-IRRAS spectral shape with monolayer compression. We have then refined the simulations by attributing a width at a half-intensity of 30 cm^{-1} for the main band and 50 cm^{-1} for the other components (with the same band shape). Fig. 9 shows that the intensity of the amide I band is best fitted with a tilt angle of 30° to the normal of the film. Using the same conditions for the optical indices ($\beta^{5.6a}$, tilt angle of 30° , and surface pressure of 40 mN m^{-1}), we have calculated the PM-IRRAS spectrum of VGA on H_2O . The comparison between the simulated and the experimental spectra (Fig. 10) shows large discrepancies: the intensity of the amide I band of the experimental spectrum is lower, and the high-frequency region (between 1650 and 1750 cm^{-1}) of this spectrum presents a completely different shape compared with the simulated spectrum. These discrepancies show that the model used, a VGA monolayer on an isotropic water subphase, is probably too simple.

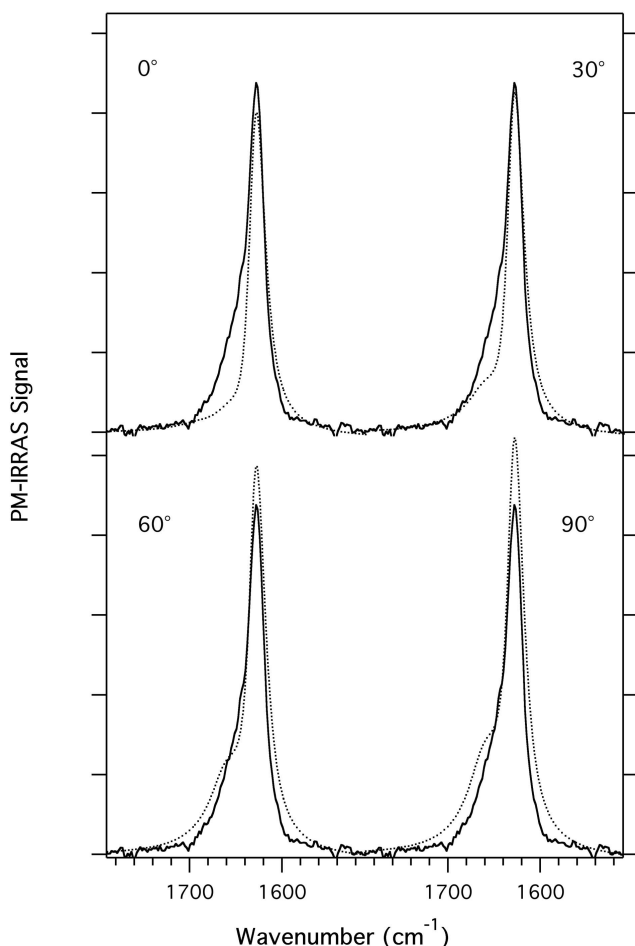


FIGURE 9 Comparison between the simulated and the experimental spectra of gramicidin and intensity comparison of the simulated spectra with the experimental spectra at 40 mN m^{-1} on D_2O at different angles with respect to the normal.

DISCUSSION

The first aim of this paper was to use the simple aliphatic peptide gramicidin to facilitate the analysis of the unfolding-folding process taking place upon spreading and compression of membrane proteins in monolayers at the air-water interface. The second aim was to determine the structure and orientation of gramicidin along its surface pressure isotherm. At large molecular area, the spread monolayer at the air-water interface is most likely unfolded. This was first proposed by Ries and Swift (1987) based on observations of the π -A isotherm. Indeed, they pointed out that the isotherm at low surface pressures yields an area per amino acid of $\sim 0.25 \text{ nm}^2$, proposing that the VGA molecules lie flat, presumably with polar groups immersed in the water and the hydrophobic moieties extending at the interface. The film thickness obtained from the reflectivity ($6\text{--}9 \text{ \AA}$; Fig. 3) strongly supports this view. Indeed, this film thickness is significantly smaller than any dimension of the

folded molecule (the smaller dimension of VGA being $\sim 15\text{--}16 \text{ \AA}$ on the basis of the crystal structure). In addition, no signal that is associated with the in-plane ordering in the film is observed with XGID below $\sim 20 \text{ mN m}^{-1}$. This is consistent with the lack of internal organization in the polypeptide (helical conformation). The folded polypeptide is known to be highly hydrophobic and, as such, would have a tendency to aggregate into partially ordered clusters, as seen with similar systems (Fukuto et al., 1997). In these studies, the XGID signal caused by the short-range order is observed at all surface pressures (Fukuto et al., 1997). This view of an almost unfolded polypeptide at large molecular areas is also evidenced by PM-IRRAS, where the amide I band is very broad and shifted from the position that is associated with any of the known β -helical conformations of VGA as well as by the observation of an efficient exchange of N-H to N-D on D_2O . Indeed, when VGA is spread on a D_2O subphase, a complete exchange of hydrogen by deuterium in the backbone of the peptide (N-H to N-D) takes place as evidenced by the large shift in the amide II band (compare Figs. 5 and 6). Such an efficient exchange is possible only if the hydrophilic moieties are immersed in water and if the polypeptide is unfolded.

The conformation of the polypeptide changes with compression of the monolayer to reach a stable conformation after the shoulder in the π -A isotherm and thus clearly shows that folding of gramicidin is taking place upon compression. In fact, the gradual transformation of the secondary structure of VGA is terminated at 15 mN m^{-1} (1.5 nm^2 permolecule) where polypeptides in the film take the tubular shape with a β -helical conformation. The PM-IRRAS data and the simulation of the spectra strongly suggest that the secondary structure of VGA at high surface pressure consists of antiparallel intertwined $\beta^{5,6}$ helices. This structure is stable above 20 mN m^{-1} and undergoes a reorientation from 90° to 30° with respect to the normal at high surface pressure as schematically presented in Fig. 11. This view is supported by the XGID measurements that show Bragg reflection associated with short-range order of VGA molecules only above a threshold pressure of 20 mN m^{-1} (Fig. 4). This result is a good demonstration of the potential of XGID for a structural determination approach of membrane-associated polypeptides (Haas et al., 1995; Verclas et al., 1999; Lenne et al., 2000). Above 15 mN m^{-1} , the behavior of the isotherm resembles that of a lipid that reorients upon compression and where the hydrophobic alkyl tails become densely packed.

The data also suggest that the VGA monolayer, at high surface pressure, induces the formation of an intermediate layer of water between the monolayer and the subphase water with characteristics that are different from those of bulk water. Indeed, an interesting result is the observation of an extra layer sandwiched between VGA and the bulk water at high surface pressures (see Fig. 2 B). The electron density in this slab ($\sim 10 \text{ \AA}$ thick) is just slightly higher than that of

F11

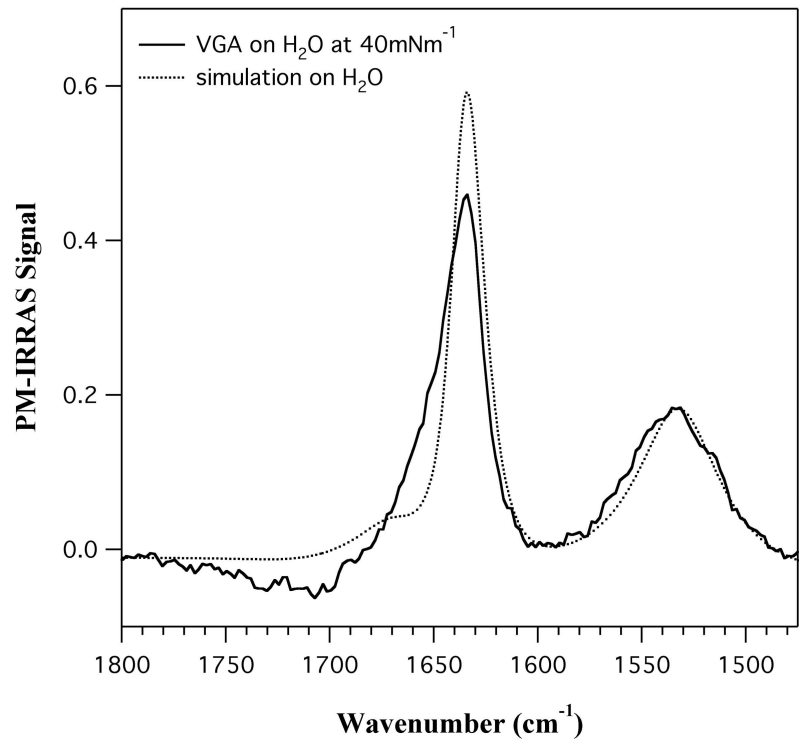


FIGURE 10 Comparison between the simulated and the experimental spectra at 40 mN m^{-1} on H_2O using the same parameters as those used on D_2O .

bulk water. This layer may be composed of a restructured film of water, and this restructuring could be induced by the

densely packed VGA. The presence of structured water underneath the film of VGA at high surface pressure is

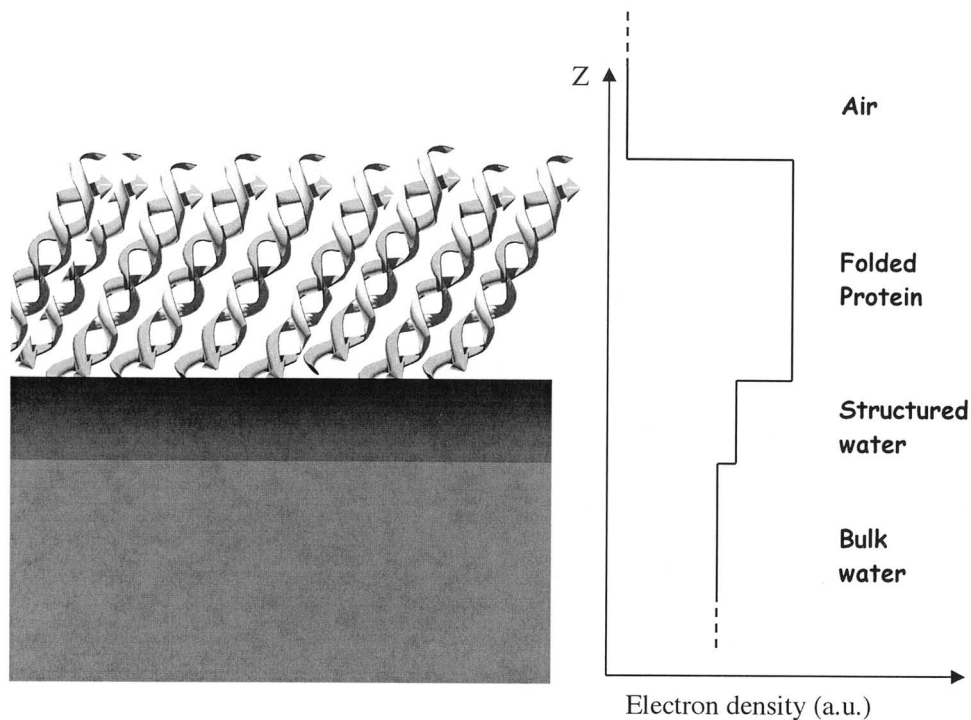


FIGURE 11 Schematic representation of VGA in monolayers at the air-water interface. VGA adopts an antiparallel double strand intertwined $\beta^{5,6}$ -helical conformation with a 30° orientation with respect to the normal with a thickness of 25 \AA . The possible presence of structured water is also represented in this figure together with the box model from the x-ray reflectivity data.

supported by the XGID and the PM-IRRAS data. The d -spacing corresponding to the second XGID weak diffraction peak $2\pi/Q_{xy}^1 = 5.43 \text{ \AA}$, with a correlation of $\sim 15 \text{ \AA}$, is characteristic of an amorphous system. This d -spacing is approximately twice the average O-O distance of 2.76 \AA in water. Based on that and on the extra layer observed in the reflectivity, one can hypothesize that this broad reflection is caused by the restructuring of water underneath the VGA film with clusters of water with an approximate diameter that is twice the value of 2.76 \AA for the O-O distance in water. This diffraction pattern shows an extra broad liquid-like peak that can be associated with the formation of water clusters of 5.5 \AA in diameter. However, this high Q_z weak diffraction peak could also correspond to a higher-order peak of VGA. In fact, given the large width of this peak (compared with the first peak; see Fig. 4), it could consist of two to three partially overlapping diffraction peaks. However, one rarely (or never) observes higher-order Bragg reflections from alkyl chains. When the structure is hexagonal, one sees the fundamental peak and nothing more. Because the linewidth is very different for the two peaks (Fig. 4), we suggest they must come from different entities: one is VGA; the other one could be restructured water. In addition, the PM-IRRAS spectral simulations on H_2O also suggest the presence of such an intermediate layer. Indeed, the discrepancies between the simulated and the experimental spectra of VGA on water suggest that the model used, a VGA monolayer on an isotropic water subphase, is probably too simple and that a structured water layer might be present underneath the VGA monolayer as proposed from the x-ray reflectivity findings. We thus propose three possible hypotheses to explain the observation of one additional slab of higher electron density, the high Q_z weak diffraction peak, and the discrepancy between the simulated and the experimental PM-IRRAS spectra of VGA on water: 1) the presence of a layer of ordered water, 2) the presence of a layer of anisotropic water (where water molecules bear a preferential orientation), or 3) a layer of water with a higher refractive index and thus a higher density than bulk water. The possible presence of such a layer of water is schematically presented in Fig. 11.

We are indebted to the Natural Sciences and Engineering Research Council of Canada for financial support. H.L. also thanks SPPUQTR and FUQTR for their financial support. C.S. is a chercheur-boursier national of the FRISQ. Ames Laboratory is operated for the U.S. Department of Energy by Iowa State University under contract W-7405-Eng-82. The work at Ames was supported by the Director for Energy Research, Office of Basic Energy Sciences.

REFERENCES

- Als-Nielsen, J., and K. Kjaer. 1989. Phase transitions in soft condensed matter. *Proc. NATO Adv. Study Inst.* 211:113–138.
- Als-Nielsen, J., and P. S. Pershan. 1983. Synchrotron x-ray diffraction study of liquid surface. *Nuclear Instrum. Methods.* 208:545–548.
- Bertie, J. E., M. K. Ahmed, and H. H. Eysel. 1989. Infrared intensities of liquids. V. Optical and dielectric constants, integrated intensities, and dipole moment derivatives of H_2O and D_2O at $22^\circ C$. *J. Phys. Chem.* 93:2210–2218.
- Blaudez, D., F. Boucher, T. Buffeteau, B. Desbat, M. Grandbois, and C. Salessse. 1999. Determination of the anisotropic optical constants of bacteriorhodopsin in the mid infrared. *Appl. Spectrosc.* 53:1299–1304.
- Blaudez, D., T. Buffeteau, J. C. Cornut, B. Desbat, N. Escafre, M. Pezolet, and J. M. Turllet. 1993. Polarization-modulated FT-IR spectroscopy of a spread monolayer at the air-water interface. *Appl. Spectrosc.* 47: 869–874.
- Blaudez, D., J.-M. Turllet, J. Dufourcq, D. Bard, T. Buffeteau, and B. Desbat. 1996. Investigation at the air/water interface using polarization modulation IR spectroscopy. *J. Chem. Soc. Faraday Trans.* 92:525–530.
- Buffeteau, T., D. Blaudez, E. Pere, and B. Desbat. 1999. Optical constant determination in the infrared of uniaxially oriented monolayers from transmittance and reflectance measurements. *J. Phys. Chem. B.* 103: 5020–5027.
- Castano, S., B. Desbat, and J. Dufourcq. 2000. Ideally amphipathic beta-sheeted peptides at interfaces: structure, orientation, affinities for lipids and hemolytic activity of (KL)(m)K peptides. *Biochim. Biophys. Acta.* 1463:65–80.
- Castano, S., B. Desbat, M. Laguerre, and J. Dufourcq. 1999. Structure, orientation and affinity for interfaces and lipids of ideally amphipathic lytic LiKj(i = 2j) peptides. *Biochim. Biophys. Acta.* 1416:176–194.
- Cornut, I., B. Desbat, J. M. Turllet, and J. Dufourcq. 1996. In situ study by polarization modulated Fourier transform infrared spectroscopy of the structure and orientation of lipids and amphipathic peptides at the air-water interface. *Biophys. J.* 70:305–312.
- Dhathathreyan, A., U. Baumann, A. Muller, and D. Mobius. 1988. Characterization of complex gramicidin monolayers by light reflection and Fourier transform infrared spectroscopy. *Biochim. Biophys. Acta.* 944: 265–272.
- Dieudonne, D., R. Mendelsohn, R. Farid, and C. Flach. 2001. Secondary structure in lung surfactant SP-B peptides: IR and CD studies of bulk and monolayer phases. *Biochim. Biophys. Acta.* 1511:99–112.
- Dluhy, R., and R. Mendelsohn. 1988. Emerging techniques in biophysical FT-IR. *Anal. Chem.* 60:269A–278A.
- Dluhy, R., K. Reilly, R. Hunt, M. Mitchell, A. Mautone, and R. Mendelsohn. 1989. Infrared spectroscopic investigations of pulmonary surfactant: surface film transitions at the air-water interface and bulk phase thermotropism. *Biophys. J.* 56:1173–1181.
- Ducharme, D., D. Vaknin, M. Paudler, C. Salessse, H. Riegler, and H. Möhwald. 1996. Surface properties of valine-gramicidin A at the air/water interface: thin solid film 284–285:90–93.
- Flach, C., J. Brauner, J. Taylor, R. Baldwin, and R. Mendelsohn. 1994. External reflection FTIR of peptide monolayer films in situ at the air/water interface: experimental design, spectra-structure correlations, and effects of hydrogen-deuterium exchange. *Biophys. J.* 67:402–410.
- Flach, C., F. Prendergast, and R. Mendelsohn. 1996. Infrared reflection-absorption of melittin interaction with phospholipid monolayers at the air/water interface. *Biophys. J.* 70:539–546.
- Fukuto, M., K. Penanen, R. K. Heilmann, P. S. Pershan, and D. Vaknin. 1997. C60-propylamine adduct monolayers at the gas/water interface: a Brewster angle microscopy and x-ray scattering study. *J. Chem. Phys.* 107:5531–5546.
- Gallant, J., B. Desbat, D. Vaknin, and C. Salessse. 1998. Polarization-modulated infrared spectroscopy and x-ray reflectivity of photosystem II core complex at the gas-water interface. *Biophys. J.* 75:2888–2899.
- Gidalevitz, D., Z. Huang, and S. Rice. 1999. Protein folding at the air-water interface studied with x-ray reflectivity. *Proc. Natl. Acad. Sci. U.S.A.* 96:2608–2011.
- Goormaghtigh, E., V. Cabiaux, and J. M. Ruysschaert. 1990. Secondary structure and dosage of soluble and membrane proteins by attenuated total reflection Fourier-transform infrared spectroscopy on hydrated films. *Eur. J. Biochem.* 193:409–420.
- Grandbois, M., B. Desbat, and C. Salessse. 2000. Monitoring of phospholipid monolayer hydrolysis by phospholipase A2 by use of polarization-

AQ: C

AQ: D

- modulated Fourier transform infrared spectroscopy. *Biophys. Chem.* 88:127–135.
- Haas, H., G. Brezesinski, and H. Mohwald. 1995. X-ray diffraction of a protein crystal anchored at the air/water interface. *Biophys. J.* 68:312–314.
- Hladky, S. B., and D. A. Haydon. 1972. Ion transfer across lipid membranes in the presence of gramicidin A. I. Studies of the unit conductance channel. *Biochim. Biophys. Acta.* 274:294–312.
- Kemp, G., and C. Wenner. 1976. Solution, interfacial, and membrane properties of gramicidin A. *Arch. Biochem. Biophys.* 176:547–555.
- Killian, J. A. 1992. Gramicidin and gramicidin-lipid interactions. *Biochim. Biophys. Acta.* 1113:391–425.
- Langs, D. A. 1988. Three-dimensional structure at 0.86 Å of the uncomplexed form of the transmembrane ion channel peptide gramicidin A. *Science.* 241:188–191.
- Lavoie, H., J. Gallant, M. Grandbois, D. Blaudez, B. Desbat, F. Boucher, and C. Salesse. 1999. The behavior of membrane proteins in monolayers at the gas-water interface: comparison between photosystem II, rhodopsin and bacteriorhodopsin. *Mater. Sci. Eng. C.* 10:147–154.
- Lenne, P. F., B. Berge, A. Renault, C. Zakri, C. Venien-Bryan, S. Courty, F. Balavoine, W. Bergsma-Schutter, A. Brisson, G. Grubel, N. Boudet, O. Konovalov, and J. F. Legrand. 2000. Synchrotron radiation diffraction from two-dimensional protein crystals at the air/water interface. *Biophys. J.* 79:496–500.
- LoGrasso, P. V., F. D. Moll, and T. A. Cross. 1988. Solvent history dependence of gramicidin A conformations in hydrated lipid bilayers. *Biophys. J.* 54:259–267.
- MacRitchie, F. 1978. Proteins at interfaces. *Adv. Protein Chem.* 32:283–326.
- MacRitchie, F. 1986. Spread monolayers of proteins. *Adv. Colloid Interface Sci.* 25:341–385.
- Mau, N. D., P. Daumas, D. Lelievre, Y. Trudelle, and F. Heitz. 1987. Linear gramicidins at the air-water interface. *Biophys. J.* 51:843–845.
- Naik, V. M., and S. Krimm. 1986. Vibrational analysis of the structure of gramicidin A. I. Normal mode analysis. *Biophys. J.* 49:1131–1145.
- Quist, P. O. 1998. ¹³C solid-state NMR of gramicidin A in a lipid membrane. *Biophys. J.* 75:2478–2488.
- Ries, H. E., and H. Swift. 1987. Monolayers of two transmembrane channel formers and an ionophore. *J. Colloid Interface Sci.* 117:584–588.
- Salemme, F. R. 1988. Structural polymorphism in transmembrane channels. *Science.* 241:145–230.
- Sarges, R., and B. Witkop. 1965. Gramicidin A. V. The structure of valine- and isoleucine-gramicidin A. *J. Am. Chem. Soc.* 87:2011–2020.
- Tournois, H., P. Gieles, R. Demel, J. de Gier, and B. de Kruijff. 1989. Interfacial properties of gramicidin and gramicidin-lipid mixtures measured with static and dynamic monolayer techniques. *Biophys. J.* 55:557–569.
- Ulrich, W. P., and H. Vogel. 1999. Polarization-modulated FTIR spectroscopy of lipid/gramicidin monolayers at the air/water interface. *Biophys. J.* 76:1639–1647.
- Urban, B. W., S. B. Hladky, and D. A. Haydon. 1978. The kinetics of ion movements in the gramicidin channel. *Fed. Proc.* 37:2628–2632.
- Urban, B. W., S. B. Hladky, and D. A. Haydon. 1980. Ion movements in gramicidin pores: an example of single-file transport. *Biochim. Biophys. Acta.* 602:331–354.
- Verclas, S. A., P. B. Howes, K. Kjaer, A. Wurlitzer, M. Weygand, G. Buldt, N. A. Dencher, and M. Losche. 1999. X-ray diffraction from a single layer of purple membrane at the air/water interface. *J. Mol. Biol.* 287:837–843.
- Wallace, B. A. 1986. Structure of gramicidin A. *Biophys. J.* 49:295–306.
- Wallace, B. A. 1998. Recent advances in the high resolution structures of bacterial channels: gramicidin A. *J. Struct. Biol.* 121:123–141.
- Wallace, B. A., and K. Ravikumar. 1988. The gramicidin pore: crystal structure of cesium complex. *Science.* 241:182–187.
- Wu, F., C. Flach, B. Seaton, T. Mealy, and R. Mendelsohn. 1999. Stability of annexin V in ternary complexes with Ca²⁺ and anionic phospholipids: IR studies of monolayer and bulk phases. *Biochemistry.* 38:792–799.

AQ: E

